HIGH TEMPERATURE TESTING OF ADDITIVELY MANUFACTURED MATERIALS

Lucy Waite, Dr. Yao Fu, Dr. Jie Song
Virginia Polytechnic Institute and State University, justwaitelu@vt.edu, yaof@vt.edu, jiesong@vt.edu

***Abstract* – This research aims to develop methods to determine the high temperature mechanical properties for additively manufactured (AM) materials and to determine the phase transition rates of AM materials when exposed to heat treatment at various high temperatures. To determine the high temperature mechanical properties, an image-based method is being developed to measure the strain experienced by a sample undergoing a tensile test at high applied temperatures. This method calculates the strain of a sample by tracking the deformation of applied thermally stable patterns over the course of a tensile test and comparing those deformations to the initial lengths of samples. To determine phase transitions of CoCrMo as it transforms from a FCC crystal lattice to an HCP crystal lattice as a result of heat treatment, the change in elongation of the CoCrMo is measured over the course of the heat treatment process. These changes in elongation when the CoCrMo is held at a constant high temperature are indicative of the FCC to HCP phase transition, and it was found that AM CoCrMo transitions to HCP more rapidly than conventionally manufactured CoCrMo at all heat treatment temperatures.**

INTRODUCTION

Within the aerospace industry, high temperature and corrosion resistant alloys play a significant role in providing air and spacecraft engines with the needed capabilities to reach their most optimal performance.

Inconel 718 (IN718), a nickel-based alloy, is frequently utilized in the aerospace industry for its high strength and corrosion resistance even at very high temperatures. Applications of IN718 include liquid-fueled rockets, jet engines, and high-speed airframe parts [1] where this high strength even at elevated temperatures is utilized to optimize component performance.

Cobalt-based alloys are also used in the aerospace industry for their high temperature resistant and high corrosion resistant properties. Applications of these alloys include within gas turbines and nozzle valves [2]. Cobalt-chromium-molybdenum (CoCrMo), as part of the family of Cobalt-based alloys, is also highly temperature resistant, and highly corrosion resistant as was described above. This alloy in particular is also highly wear-resistant and biocompatible, making it a frequently used alloy in the prosthetics industry as well [3]. Within the aerospace industry, CoCrMo is utilized by companies like GE for their GE Aviation LEAP Fuel Nozzle [4].

Both Inconel 718 and CoCrMo are capable of being used to manufacture components and parts using existing additive manufacturing techniques, allowing for these alloys to be formed into complex shapes and components that cannot be created with conventional manufacturing methods [4,5].

Using additive manufacturing to create components also introduces the potential to change the microstructure of their materials as compared to conventionally manufactured components [5,6]. These microstructural changes caused by additive manufacturing have the potential to change the mechanical behavior of materials, alongside changing how those materials respond to treatment processes, such as heat treating [5,6].

To explore how microstructural differences caused by additive manufacturing affect the mechanical properties of IN718 and CoCrMo, particularly at high temperatures, these experiments explore methods for performing high temperature tensile testing and characterizing material microstructural transitions following heat treatment.

THEORETICAL BACKGROUND

I. Material Microstructure

The microstructure of materials typically describes the arrangement of atoms and molecules at the microscopic level, including the arrangement of crystal grains, size and quantity of crystals, and material impurities [7]. A material's microstructure has a significant effect on the material's mechanical properties and behaviors in response to external stimuli. By understanding how to tailor and modify a material's microstructure, materials can be designed to better withstand high stress, high temperature, and high corrosion environments.

An important microstructural property of materials that can determine its macroscopic behavior is the crystal lattice structure. Common crystal lattice structures include body-centered cubic, face-centered cubic, and hexagonal close-packed (HCP). Figure 1

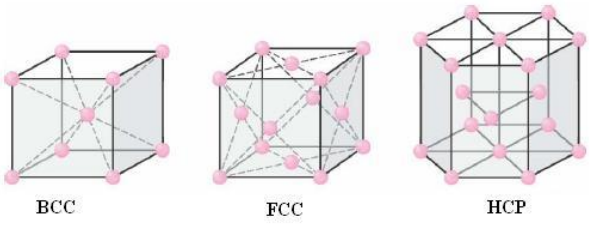

Figure 1: BCC, FCC, and HCP Material Crystal Lattice Structures

displays unit cells of these lattice patterns and how atoms are arranged within them. These crystal lattice structures form the base structural arrangement of materials at the atomic level and are stacked together to form the macroscopic materials and material properties that can be physically observed.

Elements can be arranged in several different crystal lattice structures depending on their temperature and material treatments applied. For the CoCrMo samples being studied in this research, the samples originally start in the FCC crystal lattice configuration after being initially manufactured. After being heat treated, which involves exposing samples to high temperatures for an extended period of time, the FCC CoCrMo transitions to an HCP structure. This transition in material structure has the potential to change the material's mechanical properties, which will be explored with further testing.

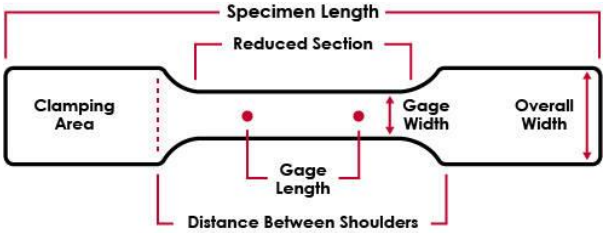

Figure 2: A dog bone sample with its defining features and dimensions labeled [9].

II. Finding the Mechanical Properties of Materials via Tensile Testing

A typical method to measure the mechanical properties of materials when tensile testing is to attach a strain gage within the gage length of a dog bone sample. These strain gages can

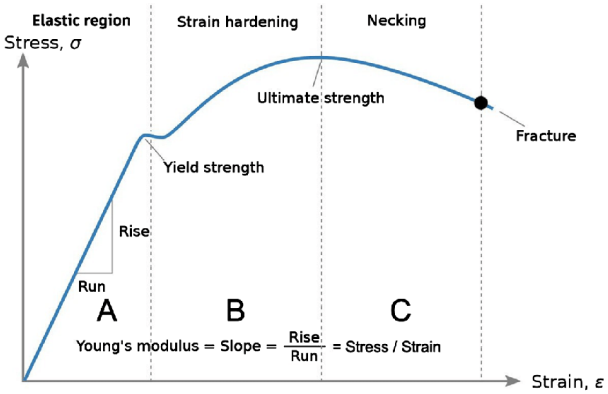

Figure 3: An example of a stress-strain curve and the mechanical properties that can be determined from it [10].

measure a sample's strain by outputting a varying electrical resistance that changes linearly with the strain experienced by the gage. A labeled image of a dog bone sample can be found in Figure 2. The gage length of dog bone sample is considered the test region when performing tensile testing, and the measured variations of the gage length are what is used to characterize the strain within the sample. For this experiment, the samples tested were all steel with a cross section of about 2mm by 1mm.

A sample's engineering strain, defined as 'ε', is calculated as follows:

$$\varepsilon = \frac{\Delta L}{L} \quad (1)$$

Where 'L' is the initial gage length, and ΔL is the change in the gage length from the initial state at any given time. During a tensile test, this measured strain is plotted against the corresponding stress applied by the tensile testing machine to the sample to define several key properties of the material. Engineering stress (σ), which is commonly used for tensile testing, is defined as follows, where 'P' is the axial tensile force exerted on the sample, and 'A' is the initial cross-sectional area of the dog bone in the gage length region prior to loading the sample:

$$\sigma = \frac{P}{A} \quad (2)$$

An example of a stress-strain diagram and the mechanical properties that can be determined from it can be seen in Figure 3. As seen in the figure, the stress-curve defines several key regions and characteristics of the material, including the material's Young Modulus ('E') (seen again in equation 3), it's yield strength (σ_Y, defined by the end of the region where stress and strain vary linearly, otherwise known as the elastic region), the ultimate strength (σ_U), and the material's strain at fracture.

$$E = \frac{\sigma}{\epsilon} \quad (3)$$

Another method for determining the strain of a material is through Digital Image Correlation (DIC). DIC uses image processing capabilities to track patterns on the surface of the dog bone sample as it undergoes a tensile test, keeping track of the number of pixels moved by points within the pattern over a given sampling period. Thereafter, the corresponding strain that the dog bone sample experienced over time can be calculated by converting the displacement of pixels to the elongation of the sample relative to its original length. This DIC process in this experiment was conducted using MATLAB and related image processing toolboxes. Similar to the strain gage, DIC used the calculated strain and plots it against the applied stress on the sample to produce the various mechanical properties previously described.

EXPERIMENTAL RESULTS

I. High-Temperature Tensile Testing of IN718

When performing tensile testing at high-temperatures, standard room temperature strain gages or other instrumentation not designed for those environments may melt or become unusable. Because of this, two different

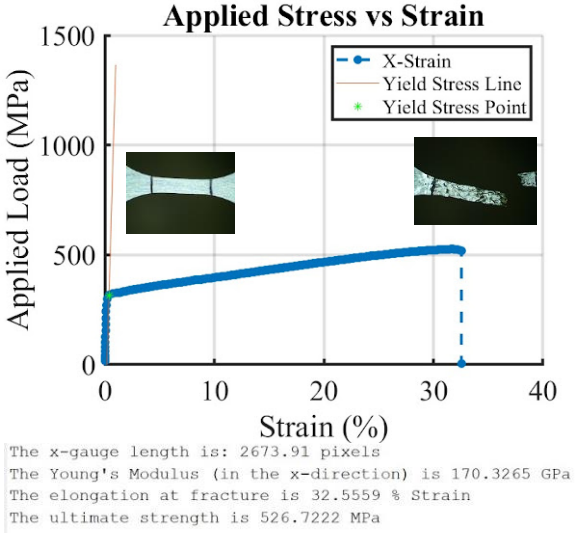

Figure 4: Example of resulting data from the modified DIC method showing the measured strain over the course of testing. The included images show the initial and final conditions of the dog bone sample.

methods were explored to test for the mechanical properties of IN718 at high temperatures:

(1) An image-based method that incorporates lens filters and a thermally stable random speckle pattern

(2) High temperature strain gages from micro-measurements attached to samples with ceramic-concrete

Both of these methods aim to mitigate the barriers posed by the high temperature test setting, with each targeting a different potential issue. The image-based method aims to mitigate the black body radiation effects caused by heating of the sample, while the high temperature strain gages combat thermal affects using more resilient metals as compared to conventionally used strain gages.

Initially, the modified DIC method was developed to be able to do high-temperature tensile testing without a significant increase in the cost and processing that would result from purchasing the high temperature strain gages and the related equipment. The experimental setup utilized a DSLR camera with a 4912 by 3684 pixel resolution, and an Instron E3000 Fatigue Testing Machine to provide the tensile force and the test framework. The images taken by the DSLR, and the forces output by the Instron machine were then imported into MATLAB to be post-processed for the material properties. An example of the code's output can be seen in Figure 4. This experimental setup was first used to test the viability of using the DSLR camera to measure strain, but modifications to the system such as the addition of blue theatrical gel filters, illuminating the sample with blue light, and utilizing bandpass filters would be needed to handle high temperature image capture. These methods would be used to mitigate the effects of thermal radiation, which emits in the infrared and red wavelength bands.

The research done up to this point ultimately found that the current set-up for image capture is not sufficient to capture the material properties within the elastic region. In materials, the elastic region typically occurs when the material's strain is below 0.2%, meaning that the sample has deformed less than 0.2% of its original length. The current setup allots approximately 2000-2500 pixels in length from the full 4912 by 3684 pixels to the initial gage length to track the samples deformations up to 50% elongation. This means that for a 0.2% deformation, only around 4-5 pixels of deformation are available to indicate behavior in the elastic region, which is not enough data to consistently produce accurate elastic region material properties. Past the elastic region, the image-based method was able to accurately and reliably produce material property data, meaning that other methods need to be explored to focus in on the elastic region and increase the number of pixels being allotted to the 0.2% deformation just for that initial stage of material testing.

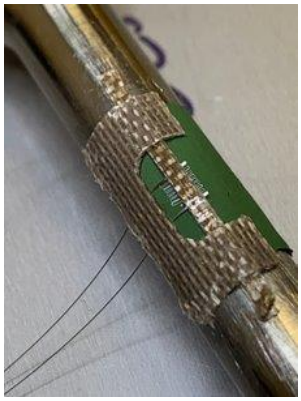

Figure 5: The ZWP Strain Gage on a Tensile Sample

While other means are explored to increase the resolution of the testing framework to accurately capture the elastic behavior, the option of using the high temperature strain gages was explored. This phase of the research found tried both the ZC-NC-1G1262-120 and ZWP-NC-063-120 strain gages and attached them to tensile samples using a thermally stable ceramic concrete. The process used to attach the strain gages with the ceramic concrete was pulled directly from the manufacturer's instructions.

This research found that the thermally stable ceramic concrete was not able to

effectively attach the strain gages to the tensile samples and ultimately sheared off before enough data could be collected for the sample's elastic region. Although capable of keeping the strain gage effectively attached for temperatures of up to 1000K, the concrete was not able to withstand the added application of stress to the sample and lead to shearing of the strain gage off the surface of the sample. Due to this shearing behavior, the high temperature strain gages and ceramic concrete will not be utilized further for the high temperature tensile testing as effective material strain data could not be collected even at room temperature.

These results indicate a need to further develop the DIC methods initially explored in order to effectively collect high temperature strain data. Some possible ways to improve the DIC method could be to:

(1) Invest in higher resolution equipment to increase the pixel count per image,

(2) Find effective ways to zoom in to a specified test region during elastic behavior testing to capture smaller deformations,

(3) Or to try tracking an applied speckle pattern instead of sectioned lines on the sample.

II. FCC to HCP Phase Transition Characterization for CoCrMo Alloy

To better understand how additively manufactured materials go through phase transition, this research explored CoCrMo's transition from the FCC to HCP lattice structure after heat treatment. This behavior was studied for both conventional and additively manufactured CoCrMo so that trans ition times could be compared for different heat treatment temperatures. The composition of the CoCrMo alloy used was Co-29Cr-5Mo. The print settings used to manufacture the additively manufactured CoCrMo alloy was a power setting of 200W and a 20μm average powder size.

This was previously explored in Donkor's paper that compared the transition times of conventional and additively manufactured CoCrMo of the same composition [11]. This research found that the additively manufactured CoCrMo sample transitioned to HCP much faster than the conventional CoCrMo samples. Donkor's work identified the material's lattice structure using X-ray diffraction (XRD), which requires an X-ray diffractometer and takes anywhere from 5-20 minutes.

This research aimed to replicate the results found by Donker by using different, more simple instrumentation and methodologies to identify the percent transition of the samples from FCC to HCP. Namely, the method aimed to characterize the phase transition by analyzing the changes in the sample's elongation throughout the heat treatment process. This elongation was measured using simple elongation probes that can withstand the high temperatures at which the samples were heat treated. Since the temperature was held constant, any changes in elongation once the sample gets up to temp can be attributed to the phase transition of the sample from FCC to HCP. Figure 6 shows an example of this phase transition and what the

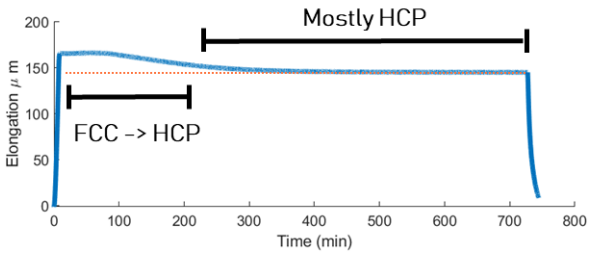

Figure 6: Sample FCC to HCP transition of CoCrMo based on elongation with heat treatment.

resulting graph would look like. The material is in the FCC phase state at the initial, higher elongation plateau, and is fully transitioned to

HCP once the elongation reduces to the lower plateau value.

This research looked at the phase transitions of heat treated conventional and additively manufactured (AM) samples of the CoCrMo at several heat treatment temperatures between 700-880 Cº. Due to the nature of high temperature testing, the quartz probes will also thermally expand during the high temperature

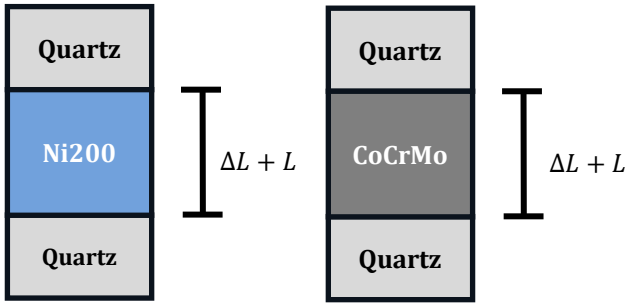

Figure 7: Testing setup for the CoCrMo and Ni200 samples with the location of the quartz sensor indicated.

heat treatment process. Due to this, a control test using Ni200 was used to characterize the quartz expansion affects that occur during the heat treatment process. A diagram showing the

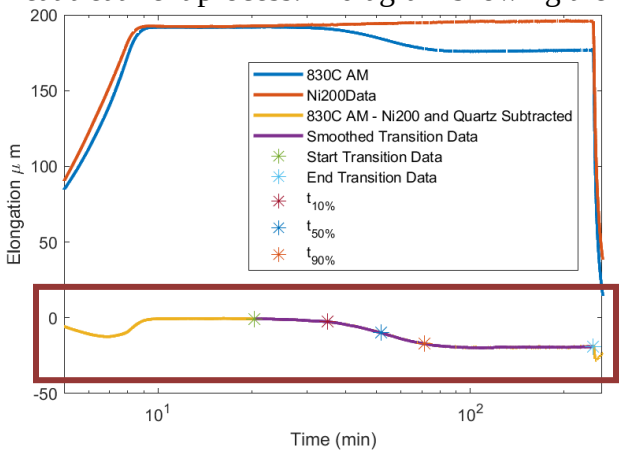

Figure 8: Phase transition data for additively manufactured CoCrMo treated at 830C.

setup and the location where elongation is measured can be found in Figure 7.

The data collected for the control Ni200 case and the CoCrMo case were subtracted from one another to get the resulting curve where the percent of transition can be extrapolated. The times for the 10%, 50% and 90% transition of FCC to HCP were extrapolated from the data by determining when the elongation reduces by 10%, 50%, and 90% of the total difference between the upper and lower plateau elongation lines. Figure 8 shows an example of this data extrapolation for the additive manufactured CoCrMo being treated at 830Cº. The boxed region on the figure shows the result after subtracting the two curves for Ni200 and CoCrMo. This curve was then smoothed to reduce noise and to pull times out more easily from the plot.

This was repeated for all the various heat treatment temperatures, and the times for 10%, 50%, and 90% were then plotted and curve-fit to find trends in transition time based on temperature. The trends for conventional and additively manufactured CoCrMo can be found in Figures 9 and Figures 10, respectfully. The trends found in these figures show that for both manufacturing methods, there is an optimal temperature for the rates of transition, and that AM CoCrMo transitions from FCC to HCP at a much higher rate than conventionally manufactured CoCrMo. This finding is validated by the findings found in Donker's paper, which also observed similar trends with AM data. This means that measuring the elongation of the sample over time is a viable method for identifying the phase transition from FCC to HCP for CoCrMo.

To further explore the phase transition of additively manufactured CoCrMo, there are plans to:

(1) Test the material properties of the HCP transitioned CoCrMo via tensile testing

(2) And to perform heat-treatment for CoCrMo manufactured with different additive manufacturing print settings to compare resulting phase transitions and material properties

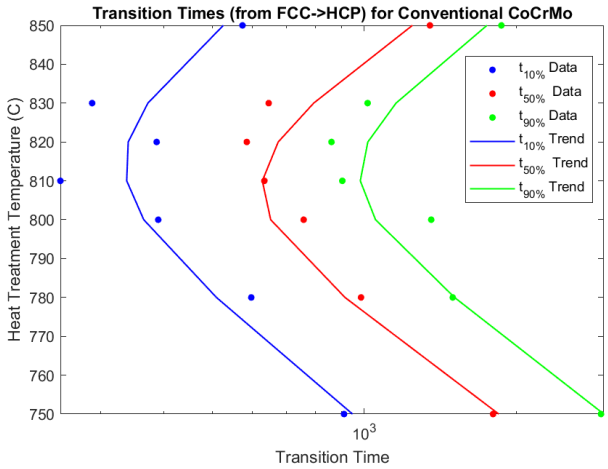

Figure 9: Conventional CoCrMo Transition Times and Trends for Several Heat Treatment Temperatures

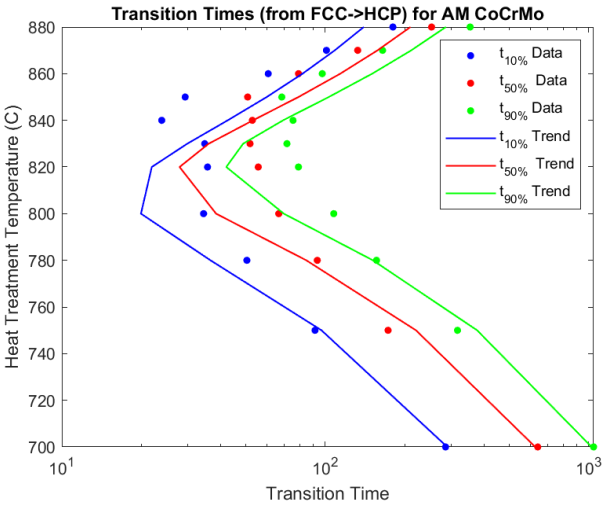

Figure 10: AM CoCrMo Transition Times and Trends for Several Heat Treatment Temperatures

CONCLUSIONS

At this time, the image-based tensile testing method for high temperatures is still a work-in-progress but has proved to be a promising method for identifying the mechanical properties of materials, especially for properties found outside of the elastic region. Further work will be done to improve the image-based method to be able to capture deformations in the elastic region, and to manage the thermal radiation resulting from high temperature testing. Once this method can is further developed, it can be used to test additively manufactured IN718 and CoCrMo alloys at high temperatures to determine how their properties differ from conventionally manufactured parts.

For the CoCrMo phase transition testing it was found that the method of characterizing phase transition by measuring changes in elongation is a viable way to determine the percent transition of CoCrMo from FCC to HCP. This was validated by comparing the results of the elongation-based transition data to that which was found by Donker [11], which used XRD analysis to determine the crystal phase transitions throughout the heat treatment process. The elongation-based transition data found that the CoCrMo samples had an ideal heat treatment temperature that made phase transition occur fastest, and that AM CoCrMo transitioned from FCC to HCP faster than if it were conventionally manufactured. These similar conclusions were also pulled from the XRD data, validating the elongation data processed in this research.

There are plans to continue this analysis of the CoCrMo alloys to understand these phase transition rates for different AM print settings, along with seeing how the mechanical properties change after phase transition for both conventional and AM samples of the CoCrMo.

REFERENCES

[1] “Inconel alloy 718 (Sept 07) Web.” Special Metals Corporation, 07-Sep-2007.
[2] “Alloy products,” Aerospace Alloys, Inc., https://www.aalloys.com/alloy-products/ (accessed Mar. 28, 2024).
[3] I. Milošev, “COCRMO alloy for biomedical applications,” *Modern Aspects*

of Electrochemistry, pp. 1–72, 2012. doi:10.1007/978-1-4614-3125-1_1
[4] General Electric, “Ge+ Cocrmo Powder Data Sheet (PDS),” General Electric, https://www.ge.com/additive/sites/default/files/2020-09/GE+PDS_CoCrMo_DMLM_r1_19Aug2020.pdf (accessed Mar. 28, 2024).
[5] E. Hosseini and V. A. Popovich, “A review of mechanical properties of additively manufactured Inconel 718,” *Additive Manufacturing*, vol. 30, p. 100877, Dec. 2019. doi:10.1016/j.addma.2019.100877
[6] Z. Liu *et al.*, “Additive Manufacturing of metals: Microstructure evolution and multistage control,” *Journal of Materials Science & Technology*, vol. 100, pp. 224–236, Feb. 2022. doi:10.1016/j.jmst.2021.06.011
[7] K. J. Kurzydłowski and B. Ralph, *The Quantitative Description of the Microstructure of Materials*. Boca Raton: CRC Press, 1995.
[8] A. Scrimshire, “Metallurgical factors influencing adhesion wear,” Degradation and Surface Engineering, https://b0039761.wordpress.com/independent-research/metallurgical-factors-influencing-adhesion-wear/ (accessed Apr. 5, 2024).
[9] ASTM D638: The Definitive Guide to Plastic Tensile testing, https://www.instron.com/en/testing-solutions/astm-standards/astm-d638 (accessed Mar. 29, 2024).
[10] A. Abdelmoez Alsayed, *A Typical Stress-Strain Curve*. 2021.
[11] B. T. Donkor *et al.*, “Accelerated γ-face-centered cubic to ε-hexagonal close packed massive transformation in a laser powder bed fusion additively manufactured co-29cr-5mo alloy,” *Scripta Materialia*, vol. 179, pp. 65–69, Apr. 2020. doi:10.1016/j.scriptamat.2020.01.012